Nuclear Inst. and Methods in Physics Research, A 942 (2019) 162384

Contents lists available at ScienceDirect

Nuclear Inst. and Methods in Physics Research, A

journal homepage: www.elsevier.com/locate/nima

Development and validation of a double focalizing magnetic spectrometer for beta spectrum measurements

Frédéric Juget [a,*], Giuseppe Lorusso [b], Guido Haefeli [c], Youcef Nedjadi [a], François Bochud [a], Claude Bailat [a]

[a] Institute of Radiation Physics, Grand Pré 1, 1007 Lausanne, Switzerland
[b] National Physics Laboratory, Hampton Road, Teddington, Middelsex TW11 0LW, United Kingdom
[c] Ecole Polytechnique Fédérale de Lausanne (EPFL), Lausanne, Switzerland

ARTICLE INFO

Keywords:
Magnetic spectrometer
Beta shape measurement
Acquisition system
^{36}Cl

ABSTRACT

In the framework of the EMPIR project MetroBeta, the development and optimization of a double focalizing magnetic spectrometer have been realized in order to measure the beta spectra shape. The acquisition is designed to perform, after focalization by the magnetic field, an energy selection using a window on the deposited energy in the Si detector. The energy calibration is performed using conversion electrons from ^{109}Cd, ^{137}Cs, ^{133}Ba and ^{207}Bi and the measured energy resolution is 1.3% at 1 MeV. The efficiency is measured experimentally using a ^{204}Tl source and is used to reconstruct the spectrum shape for beta emitters with end-point energy up to 750 keV. Two beta emitters with allowed transitions, ^{134}Cs and ^{60}Co, are used to validate the measurement and the reconstruction method. Finally the measurement of the beta shape of ^{36}Cl, a non-unique 2nd forbidden transition is presented.

1. Introduction

Precise measurement of beta spectra are increasingly important in several fields. In nuclear medicine, a better knowledge of the beta spectra is needed for the estimation of the dose induced by radiopharmaceuticals for the evaluation of the interaction with the DNA in human organs [1]. For nuclear reactors, the generation of heat upon shutdown as well as of nuclear waste is mainly due to beta decay of fission products, which requires a precise knowledge of the mean energy of the beta spectra. In fundamental research, the study of neutrinoless double beta decay studies requires a precise knowledge of the beta spectra shape for background rejection. The observed so-called "anomaly" in the anti-neutrino flux from nuclear reactors which could indicate the existence of a fourth neutrino species, also relies on the precise evaluations of beta decay [2].

In radionuclide metrology, several techniques of standardization require the knowledge of the shape of beta spectra to determine accurately the activity of beta emitters solution. The use of inappropriate beta shapes leads to discrepancies in liquid scintillation counting [3, 4]. A comparison between theoretical calculation and experimental data [5] demonstrated the need for new precise measurements of beta shapes especially beyond allowed and first forbidden transitions.

In this work and in the framework of the EMPIR Project MetroBeta [6], which aims to improve the current theoretical calculation for forbidden transitions and to measure the shape of beta spectra, the development and validation of a double focalizing magnetic spectrometer is presented. The validation is performed with the measurement of the shape of two allowed beta transitions, ^{134}Cs and ^{60}Co. Finally, the measurement spectrum of ^{36}Cl, a pure beta emitter with low intensities of X-rays, gamma and Auger electrons [7] is presented. ^{36}Cl ($T_{1/2}$ = 302(4).10^3 years) disintegrates by 98.1% to beta-minus decay to the ground state of ^{36}Ar, 1.9% to electron capture and 0.0015% to beta-plus to the ground state of ^{36}S. In this work, ^{36}Cl is considered as a pure beta emitter since all other electrons emission (Auger) are below the energy threshold. The beta minus transition is a non-unique 2nd forbidden one with a maximum energy of 706.53(5) keV [7].

The measurement of ^{36}Cl is performed with a double focalizing magnetic spectrometer described in Section 2. The sources preparation method is explained in Section 3. The execution of the experiment and the validation are described in Sections 4 and 5. The measurement results are given in Sections 6 and 7.

2. The double focalizing magnetic spectrometer

The detailed operation principle of the spectrometer is described in [8]. Basically it selects electrons using a magnetic field in both vertical and horizontal planes. The curvature of the electron trajectory at the reference radius is 18 cm and the deflection angle is 180°. The electrons are collected at the focal point on a Silicon detector. The

* Corresponding author.
E-mail address: Frederic.juget@chuv.ch (F. Juget).

https://doi.org/10.1016/j.nima.2019.162384
Received 20 May 2019; Received in revised form 9 July 2019; Accepted 14 July 2019
Available online 16 July 2019

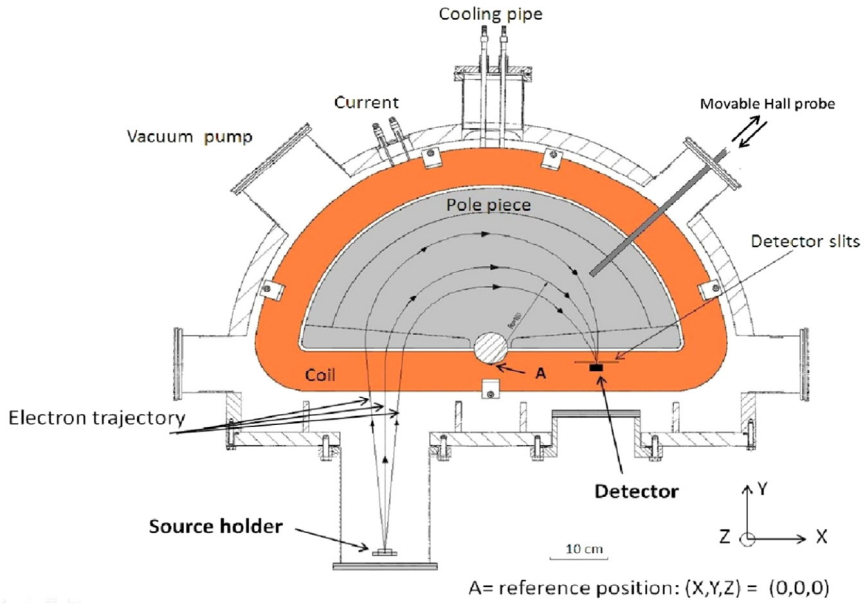

Fig. 1. Top view of the spectrometer.

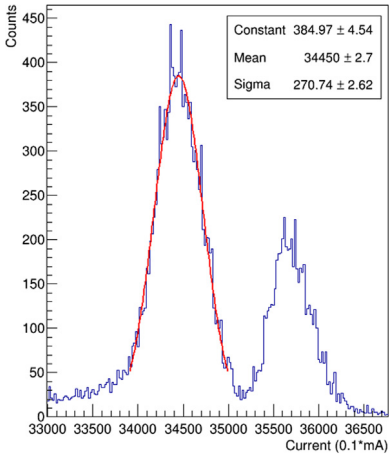

Fig. 2. Energy peak of the conversion electrons at 624.218 keV from the ^{137}Cs source versus coil current. The second peak on the right corresponds to the conversion electrons from the lines between 655.67 and 656.412 keV.

energy of the electron is selected by the magnetic field value which is controlled by the current in the coils. The magnetic field can be increased up to 0.1 T, allowing measuring a kinetic energy of the electron up to 5 MeV. The detector is a totally depleted surface barrier silicon model BA-24-50-1000 from Ortec. Its active thickness is 1 mm, which can fully stop electrons up to around 600 keV. Fig. 1 gives a schematic view of the spectrometer.

2.1. Energy calibration and resolution

The relationship between the current I and the selected electron kinetic energy T is given by the following relation, where P_0, P_1 and P_2 are parameters to be determined and m the electron mass (=511 keV) [8]:

$$\mathbf{T} = \sqrt{\mathbf{P}_0.\mathbf{I}^2 + \mathbf{P}_1.\mathbf{I} + \mathbf{P}_2} - \mathbf{m}$$

Using the conversion electrons from Cd-109 (62.5 keV), Cs-137 (624 keV), Ba-133 (45, 240, 266, 320 keV), Bi-207 (481, 975 keV) the energy calibration curve was obtained. For each energy, a representative current value I was obtained from the peak position of a Gaussian fitted to the measured energy peak (Fig. 2). The result of the calibration is given on Fig. 3 with the value of the three parameters P_0, P_1 and P_2.

The acquisition is performed using a selection on the energy deposited on the Si detector (see Section 2.2). Therefore, a relation between T (keV) and the detector output signal V (Volts) is needed. Again, using the conversion electrons and a Gaussian fit on the detector output value (Fig. 4), the signal value in Volts is obtained. Then, the curve T versus V is obtained with a linear fit (Fig. 3).

The energy resolution $\Delta T/T$ of the spectrometer is obtained using the sigma of the Gaussian fit of each electron conversion peak and is defined as the Full Width at Half Maximum, FWHM = 2.3548σ. The energy dependence of the resolution is obtained from the fit on the following relation, where p_0, p_1 and p_2 are three free parameters:

$$\frac{\Delta T}{T} = \frac{p_0}{\sqrt{T}} + \frac{p_1}{T} + p_2$$

Typically, the energy resolution at 1 MeV is of 1.3%, see Fig. 5.

2.2. The acquisition system

The deposited energy in a silicon detector will have a typical asymmetric shape as shown in Fig. 4. The peak at 0.5 Volts corresponds to the full energy deposition in the detector while the continuous tail corresponds to the backscattered or out-scattered electrons without fully depositing their energy.

In previous measurements [8], the acquisition was performed by steps in the coils current and therefore discrete kinetic energy of the electrons focalized on the detector. For each magnetic field settings, the rate was given by a direct counting of the electrons reaching the detector and depositing an energy above the electronic threshold of the acquisition system. This method is not optimal as it does not take into account the energy of the electron deposited in the detector. A new system has been developed which measures the amplitude of the signal in the detector which is proportional to the deposited electron energy and therefore allows to put a selection window on the deposited energy.

To improve measurement, only electrons which deposited their whole energy in the detector are considered. This gives a lower efficiency, but improved signal quality by reducing background. Practically, the method consists of counting only electrons which are in a window around the expected peak energy value. To implement this

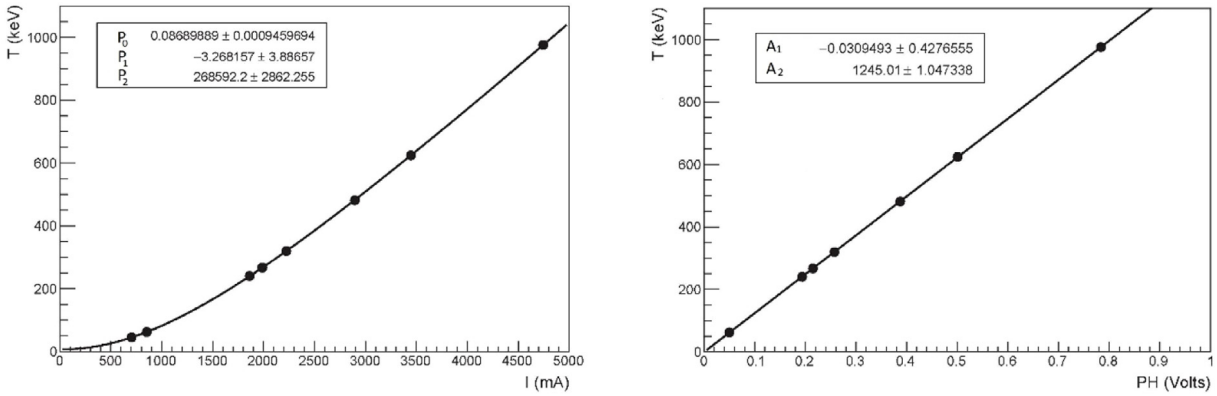

Fig. 3. Left: energy calibration curve T (keV) versus I (mA). Right: calibration curve between the kinetic energy T (keV) and pulse signal V (Volts).

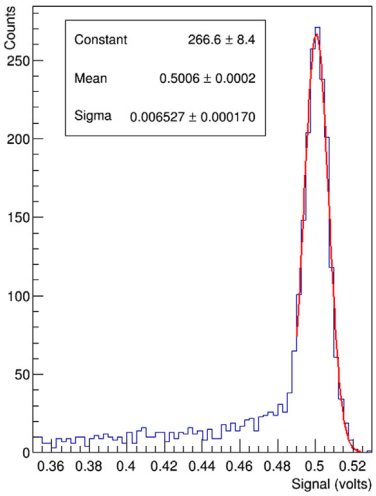

Fig. 4. Signal from the amplifier for conversion electrons of ^{137}Cs at 624 keV. The peak corresponds to the fully deposited energy and the tail on the left corresponds to the backscattered and escaping electrons.

method the relationship between the kinetic energy and the output voltage value of the detector is used (see Section 2.1).

The output voltage of the detector is recorded using a National Instrument PCI-6115 DAQ board [9], which is controlled by a home-made Labview software. This system records the maximum of the signal amplitude (in Volts), which corresponds to the deposited energy. In the case of conversion electrons, the calibration curve of Section 2 is used to convert the signal V (in Volts) into energy T (in keV).

The stored data records each electron focused in the detector and depositing a signal value V above 0.02 V, which corresponds to 25 keV.

To compute the final spectrum for a given energy, the corresponding electron number is taken as the number of electrons depositing energy inside an energy window. The size of the window must encompass the full-deposited energy peak and is fixed at 25 keV for all the energies.

For all the measurements, the spectrum is reconstructed point by point using current increments of 50 mA, starting at 850 mA, which corresponds to 62 keV. Due to the detector noise and to the electronics used to amplify the signal, it was not possible to reduce this energy threshold. An improvement can be obtained using a cooling system for the detector but such systems is not compatible with our current design.

3. Source preparation

The scattered electrons and especially the backscattered ones can enter in the spectrometer and might be focalized on the detector but with a different energy than the initial one. This will distort the initial energy spectrum to measure. The source holder is designed to avoid as much as possible the scatterings of the electrons. It consists of a square of 3 cm × 3 cm, made of 1-mm-thick Plexiglas. A hole of 1.5 cm diameter is drilled in its centre. On the bottom face, a Mylar foil of 0.5 μm thickness [10] is glued. To make the Mylar support conductive and to avoid any charges accumulation, the top face of the support is sprayed with a graphite conductive paint. On the top face, a 10 μl drop

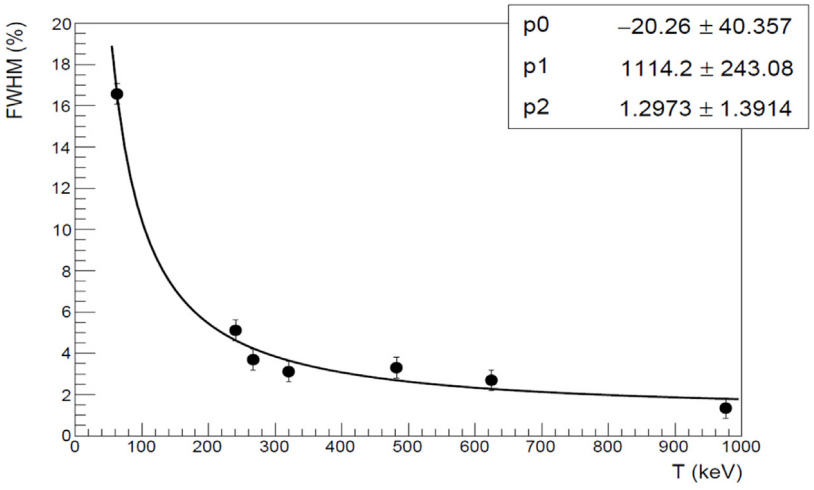

Fig. 5. Energy resolution ΔT/T measured with the conversion electrons of ^{109}Cd, ^{133}Ba, ^{137}Cs and ^{207}Bi.

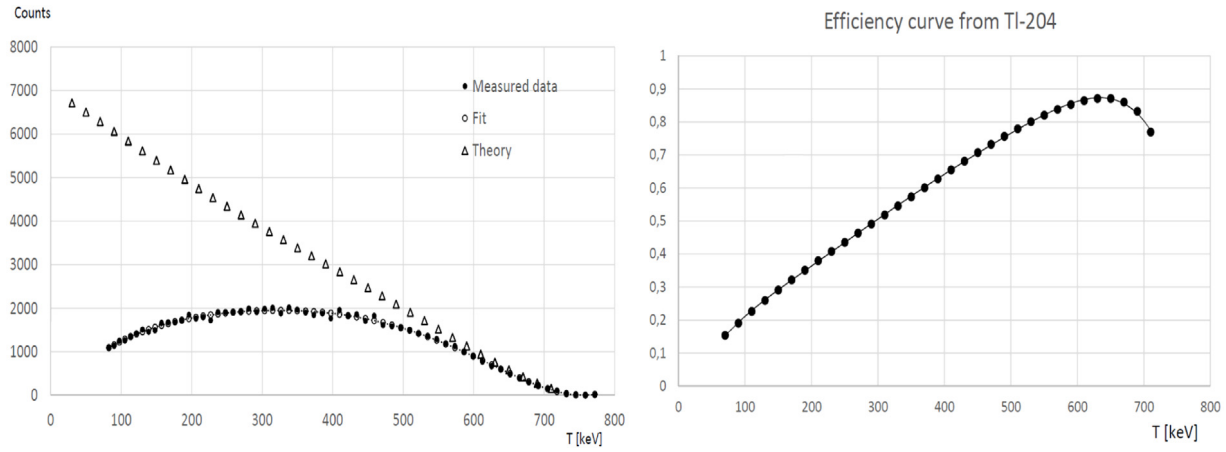

Fig. 6. Theoretical and measured spectra of ^{204}Tl (left) and measured efficiency obtained with the ratio of the two spectra.

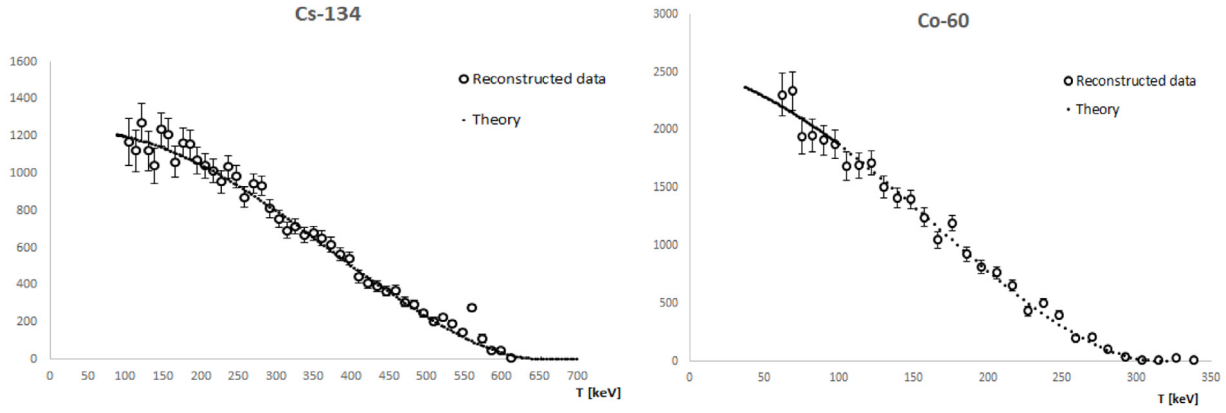

Fig. 7. Reconstructed beta spectra for ^{134}Cs and ^{60}Co using the efficiency described in Section 4.

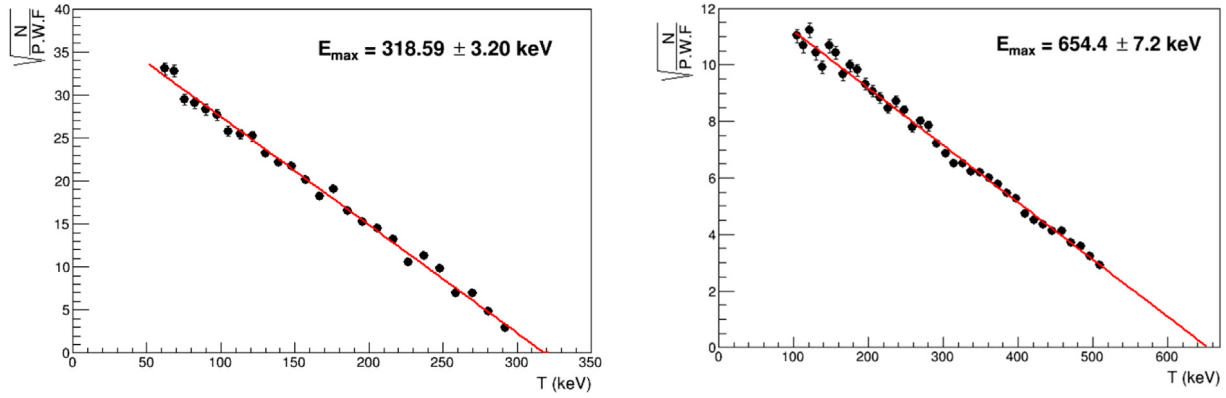

Fig. 8. Kurie plot for reconstructed data of ^{60}Co (left) and ^{134}Cs (right). For the ^{134}Cs fit, the last points (after 500 keV) have been removed since there are several conversion electrons produced in this region, which deviate the points from linearity.

of radioactive solution is deposited at the centre of the Mylar foil. Each source is weighed with a Mettler AE240 balance before and after the drop deposition to know the exact mass of the dispensed liquid and hence its activity. Then, the source is put in an airtight container with silicagel for drying. After drying, the diameter of deposited activity is under 3 mm. Normally, the radioactive solutions used to prepare the sources are in hydrochloric or aqueous form. However, the ^{36}Cl solution is with low NaCl salt concentration of around 50 mg/L in 0.00001 mol/L NaOH and a drop of 10 µl of a seeding agent, Ludox [11], diluted at 0.03%, is added before and after the radioactive drop deposition, in order to avoid to form crystals of too large thickness, which can attenuate the electron energy and distort the measured spectrum. Table 1 gives the list of the different sources prepared.

4. Efficiency

As the magnetic focalization as well as the detector efficiency are depending on the energy, the global efficiency is measured experimentally. To measure the ^{36}Cl spectrum the efficiency has to be known for an energy range up to 700 keV. To compute this efficiency, the ^{204}Tl, which is a pure beta emitter with a maximum energy of 763

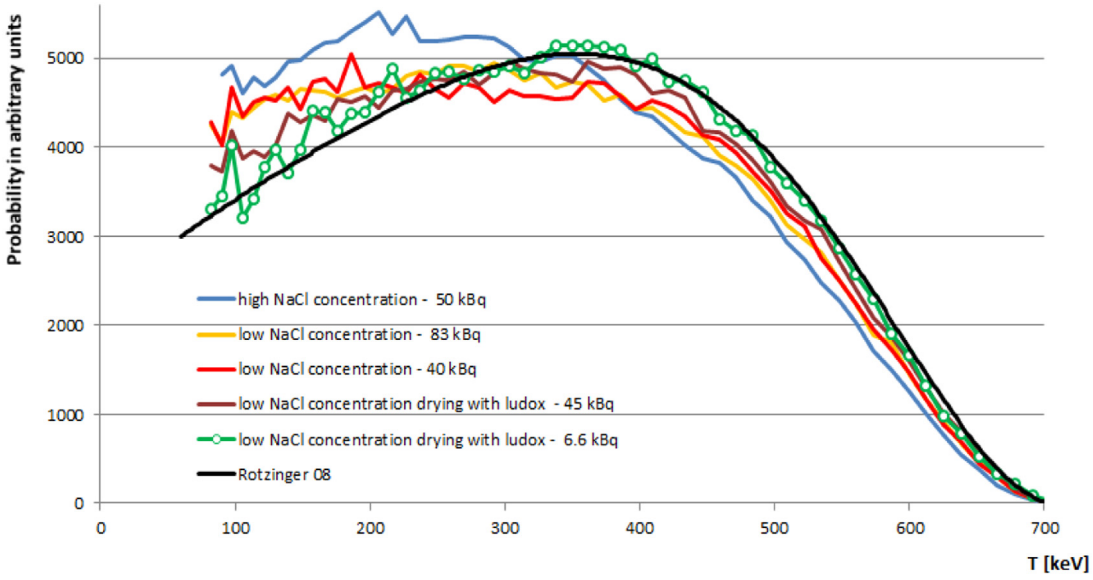

Fig. 9. Beta spectrum of ^{36}C obtained with the different sources defined in Table 2. For the low NaCl concentration, the salt quantity in the source is proportional to the activity.

Table 1
List of the sources used in this work with their activity.

Isotopes	Activity (kBq)
^{109}Cd	43 ± 1.5
^{133}Ba	64 ± 2.4
^{137}Cs	24 ± 0.4
^{207}Bi	19 ± 0.6
^{204}Tl	45 ± 2.5
^{36}Cl	6.6 ± 0.5
^{134}Cs	3.9 ± 0.3
^{60}Co	4.1 ± 0.3

Table 2
Sources used to measure effect of the amount of salt thickness on the spectrum measurement.

Source type	Activity in kBq	NaCl mass in μg
Simple drying	83	$33{\cdot}10^{-4}$
Simple drying	40	$16.5{\cdot}10^{-4}$
Drying with Ludox	45	$18{\cdot}10^{-4}$
Drying with Ludox	6.6	$2.6{\cdot}10^{-4}$

keV, is used. The obtained spectrum is given in Fig. 6 as well as the efficiency which is calculated as the ratio of the fitted curve on the experimental data and the theoretical curve calculated using the BetaShape software [12].

The curves are normalized in order to have the efficiency always below 1, as only the shape of the spectrum is considered and not on its absolute value. The obtained relative efficiency curve in Fig. 6 will be used to correct the experimental data for the ^{36}Cl spectrum.

5. Validation

In order to validate the efficiency calculation, ^{134}Cs and ^{60}Co, whose beta spectrum can be accurately calculated, because they are both allowed beta minus transitions, are measured. ^{134}Cs disintegrates by 99.58% through three allowed beta-minus transitions with maximum energy of 658.39 ± 0.33 keV. The remaining transitions are non-unique 2nd forbidden with beta energy end point at 1454 keV, which contribute little in the spectrum and can be neglected [7]. ^{60}Co disintegrates by 99.88% to an allowed beta-minus transition with energy end point at 317.32 ± 0.21 keV. The remaining transitions are unique 2nd forbidden with maximum end points at 1490 keV with low probabilities, which can be also neglected [7].

The measured spectra are given in Fig. 7. A good agreement between the reconstructed spectra using the efficiency from ^{204}Tl and the expected spectra calculated with the BetaShape software, is obtained.

The usual Fermi–Kurie plot [13] is shown in Fig. 8 to check the position of the end-point energy. The values of 318.6 ± 3.2 keV and 654.4 ± 7.2 keV are found respectively for ^{60}Co and ^{134}Cs, which are in agreement with the DDEP values [7]. The reported uncertainty contribution is only coming from the fit, which takes into account the uncertainty coming from the efficiency correction and from the statistics of each point. The fit was performed with Root software which uses a least squared minimization method [14].

6. ^{36}Cl measurement

As mentioned in Section 3, the mother solution must have a low salt content, which directly implies a low ^{36}Cl activity. Several sources were prepared with different salt concentration and ^{36}Cl activities using drying with Ludox (see Table 2). Fig. 9 shows the measured spectra for the different used sources. Increasing the amount of salt in the source, leads to more distorted spectra. The result obtained using Ludox and a low activity of about 6.6 kBq is also in reasonable agreement with the beta spectrum derived from a Magnetic Metallic Calorimeter measurement [15].

The final measured beta spectrum of ^{36}Cl was performed with the 6.6 kBq source and is presented in Fig. 10. The fit to obtain the shape factor is performed using $S(W) = 1 + AW + BW^2$ and $E_{max} = 709.55$ keV, where A and B are fit parameters and W being the electron total energy.

The obtained value, $S(W) = 1 - 1.346\ W + 0.6562\ W^2$ is in agreement with previous measurement performed with Metallic Magnetic Calorimeter [15,16] and using 4π measurement with Si detector [17]. Using this shape factor, the linear fit of the Kurie plot is used to determine the end-point energy found at 709.7 ± 3.7 keV, which is in agreement with the DDEP value; 709.53 ± 0.05 keV [7].

7. Conclusion

In this work the performance of the magnetic spectrometer, allowing the measurement of pure beta spectra with end point energy below 750 keV have been improved. The validation of the measured data

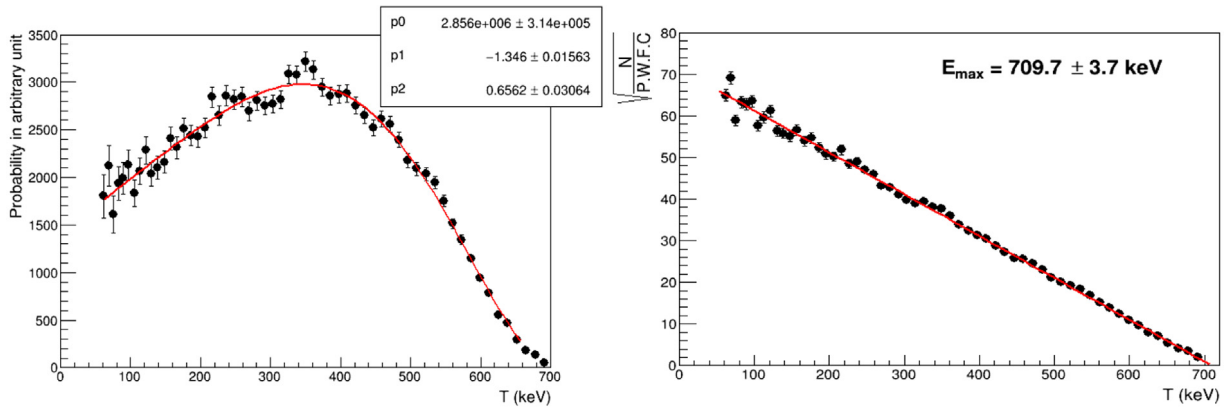

Fig. 10. Left: Reconstructed spectrum of ^{36}Cl and the fitted spectrum (line) using shape factor S(W) = 1 + A/W + B W^2. Right: Kurie plot of ^{36}Cl using the fitted shape factor.

was performed using two allowed beta transitions, ^{60}Co and ^{134}Cs, confirming the good operation of the whole set-up. The shape factor of ^{36}Cl, a non-unique 2nd forbidden transition, has been measured. The obtained result, S(W) = 1 − 1.346 W + 0.6562 W^2 is in good agreement with previous results obtained using Magnetic Metallic Calorimeter and 4π Si detector experiments. The end-point energy obtained using the Kurie plot with this shape factor is also in agreement with the DDEP value.

Despite the obtained results, the measurement uncertainties remain large and improvements have to be made, especially by taking more data points, which means reducing the current steps generating the magnetic field. A cooling system for the detector would also reduce the energy threshold, giving a measurement energy region of the beta shape spectrum more interesting for the theoretical point of view. This will also give a better stability and therefore reduce the observed fluctuation of the measurement points and therefore reduce the uncertainty of the fit parameters for the shape factor and the end point energy.

Acknowledgements

This work was performed as part of the EMPIR Project 15SIB10 MetroBeta. This project has received funding from the EMPIR programme co-financed by the Participating States and from the European Union's Horizon 2020 research and innovation programme.

This work was made possible thanks to the collaboration of the Laboratoire de Physique des Hautes Energies of the Ecole Polytechnique Fédérale de Lausanne which made available the hosting of the experiment and for its the technical support.

We would also like to thank the Physikalisch-Technische Bundesanstalt for providing us with the source of ^{36}Cl.

References

[1] M. D'Arienzo, et al., ^{90}Y PET-based dosimetry after selective internal radiotherapy treatments, Nucl. Med. Commun. 33 (6) (2012) 633–640.
[2] G. Mention, et al., Reactor antineutrino anomaly, Phys. Rev. D 83 (2011) 073006.
[3] K. Kossert, et al., Activity determination of ^{60}Co and the importance of its beta spectrum, Appl. Radiat. Isot. 134 (2018) 212–218.
[4] K. Kossert, X. Mougeot, The importance of the beta spectrum calculation for accurate activity determination of the ^{63}Ni by means of liquid scintillation, Appl. Radiat. Isot. 101 (2015) 40–43.
[5] X. Mougeot, Systematic comparison of beta spectra calculations using improved analytical screening correction with experimental shape factors, Appl. Radiat. Isot. 109 (2016) 177–182.
[6] MetroBeta EMPIR Project 15SIB10 (2016-2019), http://www.metrobeta-empir.eu/.
[7] M. Bé, et al., Table of radionuclides (Vol. 3 – A = 3 to 244). Monographie BIPM-5, Vol. 3, Bureau International des Poids et Mesures, Sèvres, ISBN: 92-822-2218-7, 2006, http://www.lnhb.fr/donnees-nucleaires/donnees-nucleaires-tableau/.
[8] F. Juget, C. Bailat, F. Bochud, Preliminary beta spectrum measurements using a magnetic spectrometer, Appl. Radiat. Isot. 87 (2014) 310–314.
[9] National Instruments, http://www.ni.com/fr-ch/support/model.pci-6115.html.
[10] Goodfellow Company, http://www.goodfellow.com see Mylar foil.
[11] Ludox product, https://www.sigmaaldrich.com/catalog/product/aldrich/420794.
[12] X. Mougeot, Reliability of usual assumptions in the calculation of β and γ spectra, Phys. Rev. C 91 (2015) Erratum Phys. Rev. 92, 059902.
[13] P. Kurie, J.R. Richardson, H.C. Paxton, The radiations emitted from artificially produced radioactive substances, Phys. Rev. 49 (1936) 368–381.
[14] Root Data Analysis Framework, https://root.cern.ch/.
[15] H. Rotzinger, M. Linck, A. Burck, M. Rodrigues, M. Loidl, E. Leblanc, L. Fleischmann, A. Fleischmann, C. Enss, Beta spectrometry with magnetic calorimeters, J. Low Temp. Phys 151 (2008) 1087–1093.
[16] K. Kossert, A. Grau Carles, O. Nähle, Čerenkov Counting and liquid scintillation counting of ^{36}Cl.LSC2010, in: Philippe Cassette (Ed.), Advances in Liquid Scintillation Spectrometry: Proceedings of the 2010 International Conference on Liquid Scintillation Spectrometry, Paris, France, 6-10 September 2010, in: Radiocarbon, the University of Arizona, Tucson, Arizona, USA, ISBN: 978-0-9638314-7-7, 2011, pp. 161–170.
[17] J.B. Willett, E.H. Spejewski, A method for resolution correction and shape factor analysis of beta spectra, Nucl. Instrum. Methods A 52 (1967) 77–85.